



HAL
open science

Double maternal effect: duplicated nucleoplasmin 2 genes, *npm2a* and *npm2b*, are shared by fish and tetrapods, and have distinct and essential roles in early embryogenesis

Caroline Cheung, Jérémy Pasquier, Aurélien Bouleau, Thuy Thao Vi Nguyen, Franck Chesnel, Yann Guiguen, Julien Bobe

► To cite this version:

Caroline Cheung, Jérémy Pasquier, Aurélien Bouleau, Thuy Thao Vi Nguyen, Franck Chesnel, et al.. Double maternal effect: duplicated nucleoplasmin 2 genes, *npm2a* and *npm2b*, are shared by fish and tetrapods, and have distinct and essential roles in early embryogenesis. 2020. hal-01608935

HAL Id: hal-01608935

<https://hal.science/hal-01608935>

Preprint submitted on 5 Jun 2020

HAL is a multi-disciplinary open access archive for the deposit and dissemination of scientific research documents, whether they are published or not. The documents may come from teaching and research institutions in France or abroad, or from public or private research centers.

L'archive ouverte pluridisciplinaire **HAL**, est destinée au dépôt et à la diffusion de documents scientifiques de niveau recherche, publiés ou non, émanant des établissements d'enseignement et de recherche français ou étrangers, des laboratoires publics ou privés.



Distributed under a Creative Commons Attribution - NonCommercial - NoDerivatives 4.0 International License

1 **Double maternal effect: duplicated nucleoplasmin 2 genes, *npm2a* and *npm2b*, are**
2 **shared by fish and tetrapods, and have distinct and essential roles in early**
3 **embryogenesis**

4 Caroline T. Cheung^(1, #), Jérémy Pasquier^(1, #), Aurélien Bouleau⁽¹⁾, Thao-Vi Nguyen⁽¹⁾, Franck
5 Chesnel⁽²⁾, Yann Guiguen⁽¹⁾, and Julien Bobe^{(1)*}

6

7 ⁽¹⁾INRA LPGP UR1037, Campus de Beaulieu, 35042 Rennes, FRANCE.

8 ⁽²⁾CNRS/ UMR6290, Université de Rennes 1, 35000 Rennes, FRANCE.

9

10 * Corresponding author E-mail: julien.bobe@inra.fr

11 Authors contributed equally to this work: #

12

13 Short Title: *npm2* genes have maternal effect in vertebrates

14 **Abstract**

15 *Nucleoplasmin 2 (npm2)* is an essential maternal-effect gene that mediates early embryonic
16 events through its function as a histone chaperone that remodels chromatin. Here we report
17 the existence of two *npm2* (*npm2a* and *npm2b*) genes in zebrafish. We examined the
18 evolution of *npm2a* and *npm2b* in a variety of vertebrates, their potential phylogenetic
19 relationships, and their biological functions using knockout models via the CRISPR/cas9
20 system. We demonstrated that the two *npm2* duplicates exist in a wide range of vertebrates,
21 including sharks, ray-finned fish, amphibians, and sauropsids, while *npm2a* was lost in
22 Coelacanth and mammals, as well as some specific teleost lineages. Using phylogeny and
23 synteny analyses, we traced their origins to the early stages of vertebrate evolution. Our
24 findings suggested that *npm2a* and *npm2b* resulted from an ancient local gene duplication,
25 and their functions diverged although key protein domains were conserved. We then
26 investigated their functions by examining their tissue distribution in a wide variety of species
27 and found that they shared ovarian-specific expression, a key feature of maternal-effect
28 genes. We also showed that both *npm2a* and *npm2b* are maternally-inherited transcripts in
29 vertebrates. Moreover, we used zebrafish knockouts to demonstrate that *npm2a* and *npm2b*
30 play essential, but distinct, roles in early embryogenesis. *npm2a* functions very early during
31 embryogenesis, at or immediately after fertilization, while *npm2b* is involved in processes
32 leading up to or during zygotic genome activation. These novel findings will broaden our
33 knowledge on the evolutionary diversity of maternal-effect genes and underlying mechanisms
34 that contribute to vertebrate reproductive success.

35

36

37 **Author Summary**

38 The protein and transcript of the *npm2* gene have been previously demonstrated as maternal
39 contributions to embryos of several vertebrates. Recently, two *npm2* genes, denoted here as
40 *npm2a* and *npm2b*, were discovered in zebrafish. This study was conducted to explore the
41 evolutionary origin and changes that occurred that culminated in their current functions. We
42 found that an ancient local duplication of the ancestral *npm2* gene created the current two
43 forms, and while most vertebrates retained both genes, notably, mammals and certain species
44 of fish lost *npm2a* and, albeit rarely, both *npm2a* and *npm2b*. Our functional analyses showed
45 that *npm2a* and *npm2b* have diverse but essential functions during embryogenesis, as *npm2a*
46 mutants failed to undergo development at the earliest stage while *npm2b* mutants developed,
47 although abnormally, until the zygotic genome activation stage after which their development
48 was arrested followed subsequently by death. Our study is the first to clearly demonstrate the
49 evolution, diversification, and functional analyses of the *npm2* genes, which are essential
50 maternal factors that are required for proper embryonic development and survival.

51

52

53 **Introduction**

54 In animals and plants, early embryonic development relies strictly on maternal
55 products until maternal-to-zygotic transition (MZT) during which zygotic genome activation
56 (ZGA) occurs [1]. Maternal-effect genes are those that are transcribed from the maternal
57 genome and whose products, which include transcripts, proteins, and other biomolecules, are
58 deposited into the oocytes during their production in order to coordinate embryonic
59 development before ZGA [2]. MZT is a key step that is needed firstly for clearance of
60 maternal components, and secondly to activate zygotic gene expression and to allow
61 subsequent embryonic development. Among the maternally-inherited transcripts that play

62 important roles during early development, some genes were demonstrated to regulate zygotic
63 program activation such as *nanog*, *pou5f1*, and *sox1* in zebrafish (*Danio rerio*) [3].
64 Henceforth, all gene and protein nomenclature will be based on that of zebrafish regardless of
65 species for simplification purposes. Those factors were shown to participate in the regulation
66 of “first wave” zygotic genes and among them, mir-430, a conserved microRNA that has
67 been shown to be involved in clearance of maternal mRNAs in zebrafish [4][5], as well as
68 mir-427, its orthologue in *Xenopus* [6]. microRNAs may also have maternal effects by
69 functioning in a similar manner to protein-coding genes, and recent revelations showed that
70 there is a subset of microRNAs that are predominantly expressed in the fish ovary and may
71 function in oogenesis and early embryogenesis [7]. Another gene, *nucleoplasmin 2* (*npm2*),
72 belongs to the family of nucleoplasmins/nucleophosmins that is maternally-inherited at both
73 protein and mRNA levels, whereby both play important roles in early development [8].
74 Historically, this protein was identified and defined as a nuclear chaperone in *Xenopus*
75 [9,10]. While the protein has been shown to be the most abundant nuclear protein in the
76 *Xenopus* oocyte [11] and to play a crucial role at fertilization due to its role in sperm
77 chromatin decondensation [12,13], its maternally-inherited mRNA has been recently
78 demonstrated to be translated as a *de novo* synthesized protein that could play a crucial role
79 during ZGA in zebrafish [8]. Further, *npm2* is one of the first identified maternal-effect genes
80 in mouse whereby its deficiency results in developmental defects and eventual embryonic
81 mortality [14].

82 The *npm2* gene belongs to the *npm* gene family that encompasses four members,
83 *npm1*, *npm2*, *npm3*, and *npm4*. The diversity of the Npm family has been shown to result
84 from the two rounds of whole genome duplication (WGD) that occurred in early vertebrates
85 (vertebrate genome duplication 1 and 2, or VGD1 & VGD2, respectively) [15,16]. Former
86 evolutionary studies clearly provided a phylogenetic model of this family; VGD1 produced two

87 genes, *npm3/2* and *npm4/1*, from an ancestral *npm* gene and the following WGD, VGD2,
88 further created the current four *npm* types with subsequent loss of *npm4* from mammals, but
89 retained in most fish species [17–20]. Recently, two *npm2* genes were automatically
90 annotated in the zebrafish genome, i.e. *npm2a* (ENSDARG00000076391) and *npm2b*
91 (previously known as *npm2*, ENSDARG00000053963). As the teleost ancestor experienced
92 an extra WGD event (TGD, or teleost-specific genome duplication) [21], doubling of genes
93 and other types of genomic rearrangement may be present in teleost species compared with
94 other vertebrates. Moreover, a fourth round of duplication occurred more recently in
95 salmonids (salmonid-specific genome duplication or SaGD) [22,23], leading to further
96 possible doubling of genes and other genomic rearrangements. As multiple evolutionary
97 events (impact of TGD, local duplication, teleost-specific duplication, etc.) could have led to
98 the *npm2a/npm2b* diversity in zebrafish, which in turn may have significant impact on
99 vertebrate reproduction, we investigated the evolution of *npm2a* and *npm2b* in a wide range
100 of vertebrate species, their potential phylogenetic relationship, as well as their biological
101 functions using transgenic zebrafish models created by the CRISPR/cas9 system in order to
102 broaden our knowledge on the evolutionary diversity of maternal-effect genes and the
103 underlying mechanisms that contribute to reproductive success in vertebrates.

104

105

106 **Results and Discussion**

107 As previously shown, *npm1*, *npm2*, *npm3* and *npm4* genes are thought to have
108 originated from the first two rounds of WGD, VGD1 and VGD2, which occurred early on in
109 vertebrate evolution [17–20]. However, two *npm2* genes have been automatically annotated
110 in the zebrafish genome, i.e. *npm2a* and *npm2b*. In order to verify if these two *npm2* genes
111 are paralogous to each other and to determine their origination, we used a Blast search

112 approach in various public databases to retrieve a multitude of sequences that could be related
113 to *npm2* genes. All retrieved sequences are compiled in Supplemental Table S1.

114

115 *Diversity of npm2a and npm2b in vertebrates*

116 Phylogenetic analysis

117 In order to verify that the retrieved protein sequences (Supplemental Table S1) were
118 homologous to zebrafish Npm2a and Npm2b, a phylogenetic analysis on Npm2 was
119 performed. Based on the alignment of 76 vertebrate Npm2-related sequences, and using
120 vertebrate Npm1 and Npm3 amino acid sequences as out-groups, a phylogenetic tree was
121 generated (Fig. 1). As shown in Fig. 1, vertebrate Npm2-related sequences clustered into two
122 clades, Npm2a and Npm2b, which were supported by significant bootstrap values, 84.2% and
123 78.2%, respectively.

124 There were 28 sequences that clustered in the Npm2a clade, which encompassed
125 sequences belonging to species from various vertebrate groups, including chondrichthyans
126 (such as dogfish Npm2a), ray-finned fish, and sarcopterygians (lobe-finned fish and
127 tetrapods). The sequences belonging to ray-finned fish included gar and bowfin Npm2a, as
128 well as teleost sequences such as zebrafish, northern pike, and rainbow trout Npm2a. In
129 contrast, no Npm2a sequence was identified in neoteleostei (medaka, European perch, and
130 Atlantic cod). The sequences belonging to sarcopterygians included amphibian (*Xenopus*)
131 Npm2a, as well as sauropsid sequences such as Chinese alligator, chicken, penguin, and ibis
132 Npm2a, although no Npm2a sequence could be identified in mammals. These results
133 provided the first evidence for the presence of orthologs to zebrafish Npm2a across
134 evolutionary divergent vertebrate groups (i.e. sauropsids, amphibians, and fish).

135 The Npm2b clade included 48 of the retrieved sequences. Like the Npm2a clade, the
136 Npm2b clade also encompassed sequences belonging to species from all of the main

137 vertebrate groups, including chondrichthyans (such as dogfish Npm2b), ray-finned fish, and
138 sarcopterygians. Ray-finned fish sequences included gar and bowfin Npm2b in addition to
139 teleost sequences such as zebrafish and northern pike Npm2b. Our analysis also demonstrated
140 the existence of two paralogous Npm2b proteins (*i.e.* Npm2b1 and Npm2b2) in all of the
141 investigated salmonid species (rainbow trout, brown trout, and brook trout). In contrast, no
142 Npm2b sequence could be identified in any neoteleostean species, including medaka, cod,
143 perch, fugu, tetraodon, and stickleback. The sequences belonging to sarcopterygians included
144 amphibian sequences such as *Xenopus* Npm2b, sauropsid sequences such as Chinese
145 alligator, ostrich, penguin and chicken Npm2b, as well as mammalian sequences such as
146 human and mouse Npm2. These results demonstrated, for the first time, that proteins
147 previously reported as Npm2 (*Xenopus*, cattle, mouse, human, zebrafish) are orthologous to
148 Npm2b in all investigated vertebrate species, and should therefore now be referred to as
149 Npm2b. In addition, with the presence of Npm2b1 and Npm2b2 in all investigated salmonid
150 species, we provided for the first time evidence of the existence of two Npm2b protein forms
151 in vertebrate species.

152 The existence of the two Npm2 clades indicated that Npm2a and Npm2b are likely
153 paralogous to each other. In addition, comparison of Npm2a and Npm2b amino acid
154 sequences in the species that harbor both revealed that they share between 30.2% and 46.4%
155 homology, depending on the species (Supplemental Table S2). The low sequence identity is
156 consistent with an ancient duplication event that gave rise to *npm2a* and *npm2b* genes.
157 However, neither the topology of the Npm2 phylogenetic tree nor the comparison between
158 Npm2a and Npm2b could indicate the kind of duplication event that had occurred. In
159 contrast, the high sequence identity shared by Npm2b1 and Npm2b2 in salmonids (between
160 75.1% and 86%) suggested a more recent duplication event. This observation in all of the

161 investigated salmonid species is consistent with the hypothesis that *npm2b1* and *npm2b2*
162 genes likely resulted from the SaGD.

163 Synteny analysis

164 In order to further understand the origin of the *npm2a* and *npm2b* genes in vertebrates,
165 we performed a synteny analysis of their neighboring genes in representative vertebrate
166 genomes. We focused our study on two mammals (human and mouse), two sauropsids
167 (Chinese alligator and chicken), two amphibians (*Xenopus tropicalis* and *laevis* L), one basal
168 sarcopterygian (coelacanth), one basal actinopterygian (spotted gar), and two teleosts
169 (zebrafish and tetraodon) (Fig. 2). Analysis was also performed on the *Xenopus laevis* S
170 subgenome, but since the results were very similar to that of *Xenopus laevis* L subgenome,
171 we only showed the latter's data [24].

172 The human, mouse, Chinese alligator, *Xenopus tropicalis* and *laevis*, coelacanth,
173 spotted gar, and zebrafish *npm2b* genes are located in genomic regions containing common
174 loci, including *dok2*, *xpo7*, *fgf17*, *dmtn*, *lgi3*, *bmp1*, *sorbs3*, *pdlim2*, *gpr124*, *prlhr*, *got11l*,
175 *adrb3*, and *nkx6-3*. Together with the phylogenetic analysis, this indicates that *npm2b* genes
176 investigated here are orthologous. Synteny analysis revealed the absence of the *npm2b* gene
177 in tetraodon although the above-mentioned neighbouring genes are present in its genome
178 (Fig. 2 and Supplemental Table S3).

179 The Chinese alligator, chicken, *Xenopus tropicalis* and *laevis*, spotted gar, and
180 zebrafish *npm2a* genes are located in genomic regions containing the same loci as *npm2b*
181 conserved regions (Fig. 2). Indeed, Chinese alligator and spotted gar *npm2a* and *npm2b* genes
182 are located in the vicinity of each other on scaffold 98.1 and the linkage group LG1,
183 respectively. The presence of *npm2a* and *npm2b* genes in the same genomic region in
184 representative species of sarcopterygians (Chinese alligator and *Xenopus tropicalis* and

185 *laevis*) and actinopterygians (spotted gar) strongly suggested that *npm2a* and *npm2b* genes
186 could have resulted from a unique local duplication of an ancestral *npm2* gene.

187

188 ***Evolutionary history of npm2 genes in vertebrates***

189 The presence/absence of *npm2a* and *npm2b* in the current vertebrate phyla and species
190 is summarized in Fig.3, and we also propose an evolutionary scenario for the diversification
191 of the *npm2* genes across vertebrate evolution.

192 In this study, we demonstrated that *npm2a* and *npm2b* may be paralogous genes
193 present in the different vertebrate groups, chondrichthyans (Fig.1), sarcopterygians, and
194 actinopterygians (Figs. 1 and 2), which strongly suggested that the *npm2* genes originated
195 from a duplication event prior to the divergence of chondrichthyans and osteichthyans. Since
196 the four *npm* family members (*npm1*, *npm2*, *npm3*, and *npm4*) are thought to be produced
197 from the first two rounds of WGD (VGD1 & VGD2) that occurred early on in vertebrate
198 evolution, we can thus hypothesize that the duplication event that generated *npm2a* and
199 *npm2b* took place after VGD2, but before emergence of chondrichthyans and osteichthyans,
200 between 450 and 500 million years ago (Mya) [25]. The findings from our synteny analysis
201 demonstrated that in representative species of actinopterygians (spotted gar) and
202 sarcopterygians (*Xenopus tropicalis* and *laevis* and Chinese alligator), *npm2a* and *npm2b*
203 genes are at two distinct loci located on the same chromosomal region (Fig. 2). These results
204 strongly suggested that *npm2a* and *npm2b* genes arose from local gene duplication rather than
205 a whole genome (or chromosome) duplication event (Fig. 3).

206 The teleost ancestor experienced an extra WGD event (TGD) [21], but in all
207 investigated teleosts, we observed a maximum of one *npm2a* ortholog and one *npm2b*
208 ortholog (except in salmonids) (Fig. 1). In addition, *npm2a* and *npm2b* are located on two
209 TGD ohnologous regions on chromosomes 8 and 10, respectively (Fig. 2), in zebrafish,

210 which is consistent with the loss of one of the *npm2a* duplicates from one region and the loss
211 of one *npm2b* duplicate from the corresponding ohnologous region. Thus, *npm2* diversity is
212 most likely due to the early loss of one of the two *npm2a* and *npm2b* TGD ohnologs (Fig. 3).
213 This observation in zebrafish strengthened the hypothesis that TGD did not impact the *npm2a*
214 and *npm2b* diversity in teleosts. In addition, the lack of *npm2a* and *npm2b* in neoteleostei
215 species, such as tetraodon, suggested that additional gene losses occurred early in the
216 evolutionary history of this group (Fig. 2).

217 In salmonids, we identified two *npm2b* paralogs, i.e. *npm2b1* and *npm2b2*, in all
218 investigated salmonid species (Fig. 1). Considering the high sequence identity shared by
219 *npm2b1* and *npm2b2*, it is strongly hypothesized that these duplicates originated from SaGD.
220 In contrast, we identified only one *npm2a* gene in all investigated salmonids suggesting that
221 SaGD did not have any impact on the current salmonid *npm2a* diversity mostly due to an
222 early loss of the SaGD ohnolog of this gene (Fig. 3).

223 In addition to the early gene losses after WGD, various other independent and
224 phylum-specific gene losses may have contributed to shape the current diversity of *npm2a*
225 and *npm2b* in vertebrates. In fact, although both *npm2a* and *npm2b* have been globally
226 conserved in sarcopterygians and actinopterygians, some phyla in each group lack at least one
227 of the genes. In sarcopterygians, *npm2a* is conserved in amphibians such as *Xenopus*
228 *tropicalis* and *laevis*, and in sauropsids such as Chinese alligator and chicken (Figs. 1-3). In
229 contrast, we did not find any *npm2a* genes in the Coelacanth genome (Figs. 1-3), which could
230 be due to the lower assembly quality of the concerned genomic region (see Supplemental
231 Table S3), and in the mammalian genomes including human and mouse (Figs. 1-3), whose
232 absence may have been due to the loss of this gene in the common ancestor of mammals. On
233 the other hand, *npm2b* is conserved in most investigated species. In actinopterygians, *npm2a*
234 and *npm2b* are both conserved in all investigated species except neoteleostei in which neither

235 *npm2a* nor *npm2b* is found. In contrast, one *npm2a* and two *npm2b*, i.e. *npm2b1* and *npm2b2*,
236 are found in salmonids, representing to date the most important diversity of *npm2* genes in
237 vertebrates (Figs. 1-3). Considering the essentialness of the *npm2* gene in embryonic
238 development, its lack in some neoteleosteon species, such as Atlantic cod and medaka, raises
239 the question on how evolution can cope with its loss. Further analyses of data from the
240 Phylofish database [26] (data not shown) showed that *npm3* had the strongest homology to
241 *npm2* and was predominantly expressed in the ovaries in medaka and cod which suggest that
242 it could potentially compensate for *npm2* deficiency. In contrast, *npm3* does not show an
243 ovarian-predominant expression in spotted gar and zebrafish, thus suggesting that its strong
244 ovarian expression could be restricted to neoteleostei.

245

246 ***Evolution of npm2a and npm2b coding sequences***

247 To examine the evolutionary adaptation of the *npm2* proteins, estimation of the ratio
248 of substitution rates (dN/dS) between the paralogous *npm2a* and *npm2b* CDS for all of the
249 species harbouring multiple *npm2* paralogs was performed (Supplemental Table S4). For all
250 investigated species, the dN/dS values were well below 1, indicating that whilst *npm2a* and
251 *npm2b* genes diverged approximately 500 Mya, they have remained under strong purifying
252 selection and evolutionary pressure, which may have tended to conserve their distinct protein
253 structures and functions. Thus, in this study, we found that Npm2a and Npm2b may have
254 diverged from an ancient duplication and currently share low sequence identity, suggesting
255 that they could have thus evolved with different roles, which were likely conserved through
256 strong negative selection.

257

258 **Expression domains of Npm2a and Npm2b in vertebrates**

259 In order to investigate further the potential functions of Npm2a and Npm2b, we first
260 explored the tissue distributions of both transcripts using two different approaches, qPCR and
261 RNA-Seq, the latter of which was obtained from the Phylofish online database [26]. In
262 zebrafish and *Xenopus tropicalis*, we observed that *npm2a* and *npm2b* were both
263 predominantly expressed in the ovary, and to a lesser extent, the muscle, as well as in the
264 zebrafish gills (Fig. 4A and 4B). We also demonstrated that *npm2a* and *npm2b* were
265 predominantly expressed in the ovary of bowfin, elephantnose fish, panga, European eel,
266 sweetfish, and northern pike (Fig. 4C to 4H). In the investigated salmonid species, brook
267 trout and brown trout, *npm2a*, *npm2b1*, and *npm2b2* were also predominantly expressed in
268 the ovary (Fig. 4I and 4J). In addition, *npm2* transcripts were expressed at a very low level in
269 the testis of European eel, northern pike, and salmonid species (Fig. 4F, 4H, 4I, and 4J). In
270 teleosts, *npm2a* mRNA levels globally tended to be lower than *npm2b* (or *npm2b1* and
271 *npm2b2* for salmonids) (Fig. 4A and 4D-J). The clear ovarian-specific expression profiles of
272 *npm2a* and *npm2b* transcripts were conserved in all investigated species, from teleosts to
273 tetrapods. This is consistent with the *npm2b* mRNA profiles reported in the literature for
274 mouse [14], cattle [27], *Xenopus tropicalis* [28], and zebrafish [8]. Despite the long passage
275 of time since their divergence (approximately 500 Mya) [25] as demonstrated above, *npm2a*
276 and *npm2b* appeared to have conserved their ovarian-specific expression profiles, which
277 suggested that they both have roles in female reproduction and/or embryonic development.

278

279 ***Embryonic expression of npm2a and npm2b***

280 Thus, in order to delve deeper into their functions in reproduction and embryogenesis,
281 we investigated *npm2a* and *npm2b* mRNA expression during oogenesis and early
282 development in zebrafish. During zebrafish oogenesis, both *npm2a* and *npm2b* transcripts

283 were found at high levels in oocytes (Fig. 5A), and despite gradual decreases in the levels of
284 both *npm2* during oogenesis, they still can be detected at reasonable amounts in the
285 unfertilized egg (i.e. metaphase 2 oocyte) (Fig. 5B). Thereafter, *npm2a* and *npm2b* transcript
286 levels progressively decreased during embryonic development after fertilization before
287 reaching very low levels at 24 hours post-fertilization (hpf) (Fig. 5B). This suggests that both
288 mRNAs are strictly maternal (i.e. not re-expressed by the zygote), which is consistent with
289 previous studies on zebrafish *npm2a* and *npm2b* transcripts [8,29]. Their expression profiles
290 are typical features of maternally-inherited mRNAs, which highly suggested that the novel
291 *npm2a* is also a maternal-effect gene.

292

293 ***Peptidic domains of npm2 paralogs***

294 We further examined the functions of the Npm2 proteins by analysis of their protein
295 domains. To date, only the role of *npm2b* has been investigated in *Xenopus tropicalis*
296 [12,30,31], mouse [14,32], humans [33–35], cattle [27], and zebrafish [8]. As previously
297 demonstrated, *npm2b* is a maternal-effect gene whose transcripts are accumulated in the
298 growing oocyte and maternally-inherited by the zygote, where it functions as a histone
299 chaperone to decondense sperm DNA as well as reorganize chromatin, thus, it has also been
300 suggested to contribute to ZGA as well [8,14,27,28]. Npm2b is thought to be activated by
301 various post-translational modifications and homo-pentamerisation [36], and subsequently
302 interacts with chromatin by exchanging sperm-specific basic proteins with histones via its
303 core domain and acidic tracts A1, A2 and A3 [34,37–42]. However, no data is available on
304 the structure and function of Npm2a. Using a predictive approach, we identified the presence
305 of the Npm core domain, acidic tract A1, and acidic tract A2 in the various investigated
306 Npm2 sequences. The nucleoplasmin family is defined by the presence of an Npm core
307 domain, which enables oligomerization of Npm proteins, in all of its members [38,43]. We

308 were able to predict the presence of this domain in all investigated Npm2a and Npm2b
309 sequences (Supplemental Fig. S1), suggesting that Npm2a proteins could also form homo- or
310 hetero-polymers. The acidic tract domains were demonstrated to facilitate histone binding by
311 increasing the recognition and affinity for different histones [40,44]. Acidic tract A1 was
312 demonstrated to be absent from most of the Npm2b investigated so far, except *Xenopus*
313 *tropicalis* Npm2b, and acidic tract A2 was predicted to be in all investigated Npm2b apart
314 from guinea pig Npm2b and American whitefish Npm2b1 (Supplemental Fig. S1). This
315 strongly suggested that the histone and basic protein binding activity of Npm2b is mediated
316 predominantly by acidic tract A2. On the other hand, in all investigated Npm2a proteins, we
317 predicted an acidic tract A1 except in that of dogfish, zebrafish, and allis shad (Supplemental
318 Fig. S1). In contrast, only half of the investigated Npm2a proteins harbored an acidic tract
319 A2, which is additionally shorter than the one present in Npm2b proteins (Supplemental Fig.
320 S1). Our results demonstrated that all Npm2a proteins, except those of Allis shad and
321 dogfish, possess acidic tracts, which could potentially mediate histone and basic protein
322 interactions.

323

324 ***Functional analysis of npm2a and npm2b in zebrafish***

325 Lastly, we performed functional analysis of these two Npm2 proteins by genetic
326 knockout using the CRISPR/cas9 system. One-cell staged embryos were injected with the
327 CRISPR/cas9 guides that targeted either *npm2a* or *npm2b* and allowed to grow to adulthood.
328 Mosaic founder mutant females (F0) were identified by fin clip genotyping and subsequently
329 mated with wild-type (WT) males, and embryonic development of the F1 fertilized eggs was
330 recorded. Since the mutagenesis efficiency of the CRISPR/cas9 system was very high, as
331 previously described [45,46], the *npm2* genes were sufficiently knocked-out even in the
332 transgenic mosaic F0 females. This was evidenced by the substantially lower transcript levels

333 of *npm2a* and *npm2b* in the F1 embryos as compared to those from control WT pairings
334 (Fig.6A). Thus, the phenotypes of *npm2a* (n=3) and *npm2b* (n=4) mutants could be observed
335 even in the F0 generation. Since none of the mutated genes were transmissible to future
336 generations neither through the male nor the female, therefore, all of our observations were
337 obtained from the F0 generation. We observed that most of the embryos from the *npm2b*
338 mutant females underwent cellular division during the very early stages of development (1-3
339 hpf) despite a considerable number of embryos with abnormal morphology ($24.00\pm 7.84\%$
340 versus 0% in controls) (Fig.6B), which included smaller size, enlarged yolk to membrane
341 ratio, and small yolk to membrane ratio. The diameter of the embryo is demonstrated by the
342 red dotted lines at oblong and germ ring stages, which reveal the extremely reduced size of
343 *npm2a* embryos (Fig.6C). Notably, around two thirds of the embryos showed abnormal cell
344 division, even in those with normal morphology, that culminated in developmental arrest at
345 around 4 hpf following which the cells stopped dividing and appeared to regress. Thus, the
346 developmental success at 4 hpf (oblong/sphere stage) was $38.09\pm 7.31\%$ vs. $85.09\pm 4.88\%$ in
347 controls (Fig.6B and 6C [right column]). By the 24 somite stage (24 hpf), these embryos were
348 all dead while the remaining embryos that showed normal development and normal cell
349 division continued to progress normally. This finding corresponded to our previous results,
350 which showed that *npm2b*-deficient embryos targeted by morpholino arrested at 4 hpf and
351 eventually died [8].

352 On the other hand, *npm2a* mutant-derived embryos had a very low developmental
353 success even at a very early stage of growth (1 hpf) ($17.62\pm 5.06\%$ vs. $85.09\pm 4.88\%$ in
354 controls) as defined by a complete lack of cell division, and a large population of them
355 ($36.36\pm 6.98\%$ vs. 0% in controls) had an abnormal morphology (Fig.6B and 6C [middle
356 columns]). The abnormal morphology of these embryos was similar to that found in *npm2b*-
357 deficient embryos. The F1 embryos that did not undergo any cell division at 1 hpf continued

358 to display a complete lack of development at 64-cell, oblong, dome, germ ring, and finally
359 somite stages (Fig.6B [middle columns]). Similar to the *npm2b* mutant-derived embryos, the
360 *npm2a*-deficient embryos were all dead by 24 hpf while the remaining embryos that showed
361 normal development and normal cell division continued to progress normally. This novel
362 finding showed for the first time that *npm2a* is essential for early development of embryos,
363 and is therefore a crucial maternal-effect gene. Further, we demonstrated that while *npm2a*
364 and *npm2b* share similar tissue distribution, as both are found specifically in the ovaries and
365 early stage embryos, their roles are distinct and essential to embryogenesis, and one could not
366 compensate for the other. Notably, *npm2a* probably plays a major role at or immediately after
367 fertilization since the embryos are arrested before the first mitotic division, which is in line
368 with a role in sperm DNA decondensation since lack of proper processing of the paternal-
369 derived DNA would lead to developmental arrest at the earliest stage and embryonic death. In
370 contrast, *npm2b* appears to function at a later stage or other factors can replace its role in the
371 early stages as the *npm2b*-deficient embryos are capable of dividing until around 4 hpf, which
372 corresponds to previous reports [8,14]. These findings are in line with those demonstrated for
373 other maternal-effect genes in mammals, such as *mater*, *floped*, *filia*, *tle6* [47], and *bcas2*
374 [48] as well as in zebrafish, including *fue* [49] and *cellular atoll* [50], all of which function to
375 moderate the early events of fertilization and embryogenesis and their ablation leads to arrest
376 and mortality at the earliest stages of embryogenesis.

377 In consequence, the dominance of the mutant allele combined with the strong
378 maternal effect of these genes, which led to massive early embryonic mortality such that none
379 of the mutant carriers survived, very likely contributed to the lack of germline transmission of
380 the mutations despite reported heritability rates of 10-30% in CRISPR/cas9-targeted zebrafish
381 from previous studies [45,46]. This was supported by detection of the mutant allele via PCR
382 genotyping in the genome of F1 *npm2a*- and *npm2b*-deficient embryos that were

383 developmentally-arrested at the germ ring stage, but not in the surviving animals at 24 hpf
384 (Supplemental Fig.S2).

385

386 **Conclusions**

387 Since two annotated genes corresponding to *npm2*, which is known as an essential
388 maternal-effect gene in mammals and amphibians, were recently found in zebrafish, we set
389 out to investigate their evolution and function. In this study, we demonstrated that the two
390 duplicates of *npm2*, *npm2a* and *npm2b*, exist in a wide range of vertebrate species, including
391 ray-finned fish, amphibians, and bird. We also found that the mammalian *npm2* gene is in
392 fact an ortholog of *npm2b*. Using phylogeny and synteny analyses, we traced the origins of
393 those two duplicates to the early stages of vertebrate evolution. Our findings indicate that
394 *npm2a* and *npm2b* genes resulted from a local gene duplication that may have occurred
395 between VGD2 and the divergence of ray-finned fish and tetrapods (~450-500 Mya). This
396 ancient origin is in line by the low sequence identity between the two *npm2* genes, although
397 the main protein domains remain conserved. Both genes exhibit a strict ovarian expression
398 and corresponding transcripts are maternally-inherited in fish and amphibians. Moreover, we
399 demonstrated and confirmed by CRISPR/cas9-directed genetic knockout of *npm2a* and
400 *npm2b* that they are both maternal-effect genes that play essential, but distinct, roles in early
401 embryogenesis. *npm2a* probably plays a major role at or immediately after fertilization, and
402 most likely in chromatin sperm decondensation. In contrast, *npm2b* appears to function at a
403 later stage and could participate in ZGA. Our findings will help us gain further insight into
404 the evolutionary diversity of maternal-effect genes and understand the underlying
405 mechanisms that contribute to reproductive success in vertebrates.

406

407

408 **Material and Methods**

409 ***Genomic databases***

410 The following genomic data were extracted and investigated from the ENSEMBL genomic
411 database (<http://www.ensembl.org/index.html>): human, *Homo sapiens*; mouse, *Mus*
412 *musculus*; chicken, *Gallus gallus*; *Xenopus*, *Xenopus tropicalis*; coelacanth, *Latimeria*
413 *chalumnae*; spotted gar, *Lepisosteus oculatus*; zebrafish, *Danio rerio*; and tetraodon,
414 *Tetraodon nigroviridis*. The Chinese alligator (*Alligator sinensis*) genome was extracted and
415 investigated from the NCBI genomic database (<http://www.ncbi.nlm.nih.gov/genome/22419>).
416 The *Xenopus laevis* L and S genomes were analyzed from the Xenbase database
417 (www.xenbase.org).

418 ***Transcriptomic databases***

419 The following actinopterygian transcriptomes were retrieved and investigated from the
420 Phylofish database (<http://phylofish.sigene.org/index.html>): bowfin, *Amia calva*; spotted gar,
421 *Lepisosteus oculatus*; elephantnose fish, *Gnathonemus petersi*; arowana, *Osteoglossum*
422 *bicirrhosum*; butterflyfish, *Pantodon buchholzi*; European eel, *Anguilla anguilla*; rainbow
423 trout, *Oncorhynchus mykiss*; allis shad, *Alosa alosa*; zebrafish, *Danio rerio*; panga,
424 *Pangasius hypophthalmus*; northern pike, *Esox lucius*; grayling, *Thymallus thymallus*;
425 Atlantic cod, *Gadhus morua*; medaka, *Oryzias latipes*; European perch, *Perca fluviatilis*;
426 brown trout, *Salmo trutta*; European whitefish, *Coregonus lavaretus*; brook trout, *Salvelinus*
427 *fontinalis*; Astyanax, *Astyanax mexicanus*; lake whitefish, *Coregonus clupeaformis*; eastern
428 mudminnow, *Umbra pygmae*, and sweetfish, *Plecoglossus altivelis*.

429 ***Gene predictions***

430 **TBLASTN search**

431 Genomic data were analyzed using the TBLASTN algorithm (search sensitivity: near exact
432 match short) on the ENSEMBL website or the NCBI browser for the Chinese alligator

433 genome. The TBLASTN algorithm on the SIGENAE platform was used on the
434 transcriptomic data.

435 Predictions of *npm2* genes

436 The peptidic sequences of zebrafish Npm2a and Npm2b were used as query in TBLASTN
437 search to identify the open reading frame (ORF) encoding *npm2* genes in the various
438 investigated genomes and transcriptomes.

439 ***Phylogenetic analysis***

440 Amino acid sequences of 75 Npm2, 3 Npm3, and 3 Npm1 proteins were first aligned using
441 ClustalW. The JTT (Jones, Taylor, and Thornton) protein substitution matrix of the resulting
442 alignments was determined using ProTest software. Phylogenetic analysis of Npm proteins
443 was performed using the Maximum Likelihood method (MEGA 5.1 software) with 1,000
444 bootstrap replicates.

445 ***Synteny analyses***

446 Synteny maps of the conserved genomic regions in human, mouse, chicken, Xenopus,
447 coelacanth, spotted gar, zebrafish, and tetraodon were produced using PhyloView on the
448 Genomicus v75.01 website ([http://www.genomicus.biologie.ens.fr/genomicus-75.01/cgi-](http://www.genomicus.biologie.ens.fr/genomicus-75.01/cgi-bin/search.pl)
449 [bin/search.pl](http://www.genomicus.biologie.ens.fr/genomicus-75.01/cgi-bin/search.pl)). Synteny analysis of the Chinese alligator conserved genomic regions was
450 performed using TBLASTN searches in the corresponding genomic database. For each gene,
451 the peptidic sequences of human and chicken were used as query, as far as they were
452 referenced in the databases.

453 ***RNA-seq***

454 RNA-seq data were deposited into Sequence Read Archive (SRA) of NCBI under accession
455 references SRP044781-84, SRP045138, SRP045098-103, and SRP045140-146. The
456 construction of sequencing libraries, data capture and processing, sequence assembly,
457 mapping, and interpretation of read counts were all performed as previously reported with

458 some modifications [26]. In order to study the transcript expression patterns and levels of
459 *npm2* for each actinopterygian species presenting 2 or 3 *npm2* genes, we mapped the double
460 stranded RNA-seq reads to the corresponding *npm2* CDS using BWA-Bowtie with stringent
461 mapping parameters (maximum number of allowed mismatches –aln 2). Mapped reads were
462 counted using the idxstat command in SAMtools, with a minimum alignment quality value (–
463 q 30) to discard ambiguous mapping reads. For each species, the number of mapped reads
464 was then normalized for each *npm2* gene across the 11 tissues using RPKM normalization.

465 ***Quantitative real-time PCR (QPCR)***

466 For each sample, total RNA was extracted using Tri-Reagent (Molecular Research Center,
467 Cincinnati, OH) according to the manufacturer’s instructions. Reverse transcription (RT) was
468 performed using 1 µg of RNA from each sample with M-MLV reverse transcriptase and
469 random hexamers (Promega, Madison, WI). Briefly, RNA and dNTP were denatured for
470 6 min at 70°C and then chilled on ice for 5 min before addition of the RT reagents. RT was
471 performed at 37°C for 1 h and 15 min followed by a 15-min incubation step at 70°C. Control
472 reactions were run without reverse transcriptase and used as negative control in the QPCR
473 study. For each studied tissue, cDNA originating from three individual fish were pooled and
474 subsequently used for QPCR. Follicular oocytes at different stages of oogenesis were
475 obtained from at least 3 different wildtype animals, and pooled embryos were obtained from
476 at least 3 clutches from each individual mutant. QPCR experiments were performed with the
477 Fast-SYBR GREEN fluorophore kit (Applied Biosystems, Foster City, CA) as per the
478 manufacturer’s instructions using 200 nM of each primer in order to keep PCR efficiency
479 between 90% and 100%, and an Applied Biosystems StepOne Plus instrument. RT products,
480 including control reactions, were diluted 1/25, and 4 µl of each sample were used for each
481 PCR. All QPCR were performed in triplicate. The relative abundance of target cDNA was
482 calculated from a standard curve of serially diluted pooled cDNA and normalized to 18S, β-

483 actin, β -2 microglobulin, and EF1 α transcripts. The primer sequences can be found in
484 Supplemental Table S5.

485 ***Comparison of npm2a and npm2b peptidic sequences***

486 For the species harbouring Npm2a and Npm2b, or Npm2a, Npm2b1, and Npm2b2, we
487 compared the corresponding protein sequences using EMBOSS Matcher tool on the EBI
488 website (http://www.ebi.ac.uk/Tools/psa/emboss_matcher/). Results of the pair-wise
489 comparisons are presented as identity percentages in Supplemental Table S2. We also
490 estimated the synonymous substitution rates (dS) and non-synonymous substitution rates
491 (dN) between the paralogous Npm2a and Npm2b coding sequences (CDS) using JCoDA
492 v1.14 software (<http://www.tcnj.edu/~nayaklab/jcoda>). The alignment options were set to
493 “clustal”, and the Yang and Nielsen dN/dS substitution models were used.

494 ***CrispR-cas9 genetic knockout***

495 CRISPR/cas9 guide RNA (gRNA) were designed using the ZiFiT online software and were
496 made against 3 targets within each gene to generate large genomic deletions, ranging from
497 250-1600 base pairs, that span exons which allow the formation of non-functional proteins.
498 Nucleotide sequences containing the gRNA were ordered, annealed together, and cloned into
499 the DR274 plasmid. *In vitro* transcription of the gRNA from the T7 initiation site was
500 performed using the Maxiscript T7 kit (Applied Biosystems), and their purity and integrity
501 were assessed using the Agilent RNA 6000 Nano Assay kit and 2100 Bioanalyzer (Agilent
502 Technologies, Santa Clara, CA). Zebrafish embryos at the one-cell stage were micro-injected
503 with approximately 30-40 pg of each CRISPR/cas9 guide along with 8-9 nM of purified cas9
504 protein (a generous gift from Dr. Anne de Cian from the National Museum of Natural History
505 in Paris, France). The embryos were allowed to grow to adulthood, and genotyped using fin
506 clip and PCR that detected the deleted regions. The PCR bands of the mutants were then sent
507 for sequencing to verify the deletion. Once confirmed, the mutant females were mated with

508 wildtype males to produce F1 embryos, whose phenotypes were subsequently recorded.
509 Images were captured with a Carl Zeiss microscope (Jena, Germany) and TouPCam camera
510 (TouPTek, Hangzhou, China).

511 ***Genotyping by PCR***

512 Fin clips were harvested from animals under anesthesia (0.1% phenoxethanol) and lysed
513 with 5% chelex containing 100 µg of proteinase K at 55°C for 2 hrs and then 99°C for 10
514 minutes. The extracted DNA was subjected to PCR using Advantage2 system (Clontech,
515 Mountain View, CA) for *npm2b* and Jumpstart Taq polymerase (Sigma-Aldrich, St. Louis,
516 MO) for *npm2a*. The primers are listed in Supplemental Table S5.

517 ***Statistical Analysis***

518 Comparison of two groups was performed using the GraphPad Prism statistical software (La
519 Jolla, CA), and either the Student's t-test or Mann-Whitney U-test was conducted depending
520 on the normality of the groups based on the Anderson-Darling test.

521

522

523 **Acknowledgements**

524 This work was supported by ANR grants PHYLOFISH (ANR-10-GENM-017) and
525 Maternal Legacy (ANR-13-BSV7-0015) to JB. Authors would like to thank Dr. Yann Audic
526 for providing *Xenopus tropicalis* animals and Ms. Amélie Patinote for zebrafish rearing and
527 egg production.

528

529

530 **References**

531 1. Baroux C, Autran D, Gillmor CS, Grimanelli D, Grossniklaus U. The maternal to
532 zygotic transition in animals and plants. *Cold Spring Harb Symp Quant Biol.* 2008;73:

- 533 89–100.
- 534 2. Lindeman RE, Pelegri F. Vertebrate maternal-effect genes: Insights into fertilization,
535 early cleavage divisions, and germ cell determinant localization from studies in the
536 zebrafish. *Mol Reprod Dev.* 2010;77: 299–313.
- 537 3. Lee MT, Bonneau AR, Takacs CM, Bazzini AA, DiVito KR, Fleming ES, et al.
538 Nanog, Pou5f1 and SoxB1 activate zygotic gene expression during the maternal-to-
539 zygotic transition. *Nature.* 2013;503: 360–364.
- 540 4. Giraldez AJ, Mishima Y, Rihel J, Grocock RJ, Van Dongen S, Inoue K, et al.
541 Zebrafish MiR-430 promotes deadenylation and clearance of maternal mRNAs.
542 *Science.* 2006;312: 75–79.
- 543 5. Giraldez AJ. microRNAs, the cell’s Nepenthe: clearing the past during the maternal-
544 to-zygotic transition and cellular reprogramming. *Curr Opin Genet Dev.* 2010; 20:369–
545 375.
- 546 6. Lund E, Liu M, Hartley RS, Sheets MD, Dahlberg JE. Deadenylation of maternal
547 mRNAs mediated by miR-427 in *Xenopus laevis* embryos. *Rna.* 2009;15: 2351–2363.
- 548 7. Bouchareb A, Le Cam A, Montfort J, Gay S, Nguyen T, Bobe J, et al. Genome-wide
549 identification of novel ovarian-predominant miRNAs: new insights from the medaka
550 (*Oryzias latipes*). *Sci Rep.* 2017;7: 40241.
- 551 8. Bouleau A, Desvignes T, Traverso JM, Nguyen T, Chesnel F, Fauvel C, et al.
552 Maternally inherited npm2 mRNA is crucial for egg developmental competence in
553 zebrafish. *Biol Reprod.* 2014;91: 43.
- 554 9. Laskey RA, Honda BM, Mills AD, Finch JT. Nucleosomes are assembled by an acidic
555 protein which binds histones and transfers them to DNA. *Nature.* 1978;275: 416–420.
- 556 10. Laskey RA, Earnshaw WC. Nucleosome assembly. *Nature.* 1980;286: 763–767.
- 557 11. Mills AD, Laskey RA, Black P, De Robertis EM. An acidic protein which assembles

- 558 nucleosomes in vitro is the most abundant protein in *Xenopus* oocyte nuclei. *J Mol*
559 *Biol.* 1980;139: 561–568.
- 560 12. Philpott A, Leno GH, Laskey RA. Sperm decondensation in *Xenopus* egg cytoplasm is
561 mediated by nucleoplasmin. *Cell.* 1991;65: 569–578.
- 562 13. Philpott A, Leno GH. Nucleoplasmin remodels sperm chromatin in *Xenopus* egg
563 extracts. *Cell.* 1992;69: 759–767.
- 564 14. Burns KH, Viveiros MM, Ren Y, Wang P, DeMayo FJ, Frail DE, et al. Roles of
565 NPM2 in chromatin and nucleolar organization in oocytes and embryos. *Science.*
566 2003;300: 633–636.
- 567 15. Dehal P, Boore JL. Two rounds of whole genome duplication in the ancestral
568 vertebrate. *PLoS Biol.* 2005;3: e314.
- 569 16. Van de Peer Y, Maere S, Meyer A. The evolutionary significance of ancient genome
570 duplications. *Nat Rev Genet.* 2009;10: 725–732.
- 571 17. Eirin-Lopez JM, Frehlick LJ, Ausio J. Long-term evolution and functional
572 diversification in the members of the nucleophosmin/nucleoplasmin family of nuclear
573 chaperones. *Genetics.* 2006;173: 1835–1850.
- 574 18. Frehlick LJ, Eirin-Lopez JM, Jeffery ED, Hunt DF, Ausio J. The characterization of
575 amphibian nucleoplasmins yields new insight into their role in sperm chromatin
576 remodeling. *BMC Genomics.* 2006;7: 99.
- 577 19. Wotton KR, Weierud FK, Dietrich S, Lewis KE. Comparative genomics of Lbx loci
578 reveals conservation of identical Lbx ohnologs in bony vertebrates. *BMC Evol Biol.*
579 2008;8: 171.
- 580 20. Jovelin R, Yan YL, He X, Catchen J, Amores A, Canestro C, et al. Evolution of
581 developmental regulation in the vertebrate FgfD subfamily. *J Exp Zool B Mol Dev*
582 *Evol.* 2010;314: 33–56.

- 583 21. Glasauer SM, Neuhauss SC. Whole-genome duplication in teleost fishes and its
584 evolutionary consequences. *Mol Genet Genomics*. 2014;289: 1045–1060.
- 585 22. Volff JN. Genome evolution and biodiversity in teleost fish. *Heredity (Edinb)*.
586 2005;94: 280–294.
- 587 23. Berthelot C, Brunet F, Chalopin D, Juanchich A, Bernard M, Noel B, et al. The
588 rainbow trout genome provides novel insights into evolution after whole-genome
589 duplication in vertebrates. *Nat Commun*. 2014;5: 3657.
- 590 24. Session AM, Uno Y, Kwon T, Chapman JA, Toyoda A, Takahashi S, et al. Genome
591 evolution in the allotetraploid frog *Xenopus laevis*. *Nature*. 2016;538: 336–343.
- 592 25. Near TJ, Eytan RI, Dornburg A, Kuhn KL, Moore JA, Davis MP, et al. Resolution of
593 ray-finned fish phylogeny and timing of diversification. *Proc Natl Acad Sci U S A*.
594 2012;109: 13698–13703.
- 595 26. Pasquier J, Cabau C, Nguyen T, Jouanno E, Severac D, Braasch I, et al. Gene
596 evolution and gene expression after whole genome duplication in fish: the PhyloFish
597 database. *BMC Genomics*. 2016;17: 368.
- 598 27. Lingenfelter BM, Tripurani SK, Tejomurtula J, Smith GW, Yao J. Molecular cloning
599 and expression of bovine nucleoplasmin 2 (NPM2): a maternal effect gene regulated
600 by miR-181a. *Reprod Biol Endocrinol*. 2011;9: 40.
- 601 28. Burglin TR, Mattaj IW, Newmeyer DD, Zeller R, De Robertis EM. Cloning of
602 nucleoplasmin from *Xenopus laevis* oocytes and analysis of its developmental
603 expression. *Genes Dev*. 1987;1: 97–107.
- 604 29. Harvey SA, Sealy I, Kettleborough R, Fenyes F, White R, Stemple D, et al.
605 Identification of the zebrafish maternal and paternal transcriptomes. *Development*.
606 2013;140: 2703–2710.
- 607 30. Laskey RA, Mills AD, Philpott A, Leno GH, Dilworth SM, Dingwall C. The role of

- 608 nucleoplasmin in chromatin assembly and disassembly. *Philos Trans R Soc Lond B*
609 *Biol Sci.* 1993;339: 263–269.
- 610 31. Prado A, Ramos I, Frehlick LJ, Muga A, Ausio J. Nucleoplasmin: a nuclear chaperone.
611 *Biochem Cell Biol.* 2004;82: 437–445.
- 612 32. De La Fuente R, Viveiros MM, Burns KH, Adashi EY, Matzuk MM, Eppig JJ. Major
613 chromatin remodeling in the germinal vesicle (GV) of mammalian oocytes is
614 dispensable for global transcriptional silencing but required for centromeric
615 heterochromatin function. *Dev Biol.* 2004;275: 447–458.
- 616 33. Lee HH, Kim HS, Kang JY, Lee BI, Ha JY, Yoon HJ, et al. Crystal structure of human
617 nucleoplasmin-core reveals plasticity of the pentamer-pentamer interface. *Proteins.*
618 2007;69: 672–678.
- 619 34. Platonova O, Akey I V, Head JF, Akey CW. Crystal structure and function of human
620 nucleoplasmin (npm2): a histone chaperone in oocytes and embryos. *Biochemistry.*
621 2011;50: 8078–8089.
- 622 35. Okuwaki M, Sumi A, Hisaoka M, Saotome-Nakamura A, Akashi S, Nishimura Y, et
623 al. Function of homo- and hetero-oligomers of human nucleoplasmin/nucleoplasmin
624 family proteins NPM1, NPM2 and NPM3 during sperm chromatin remodeling.
625 *Nucleic Acids Res.* 2012;40: 4861–4878.
- 626 36. Onikubo T, Nicklay JJ, Xing L, Warren C, Anson B, Wang WL, et al.
627 Developmentally Regulated Post-translational Modification of Nucleoplasmin
628 Controls Histone Sequestration and Deposition. *Cell Rep.* 2015. pii:S2211-
629 1247(15)00196-5. doi: 10.1016/j.celrep.2015.02.038.
- 630 37. Dingwall C, Dilworth SM, Black SJ, Kearsey SE, Cox LS, Laskey RA. Nucleoplasmin
631 cDNA sequence reveals polyglutamic acid tracts and a cluster of sequences
632 homologous to putative nuclear localization signals. *Embo J.* 1987;6: 69–74.

- 633 38. Dutta S, Akey I V, Dingwall C, Hartman KL, Laue T, Nolte RT, et al. The crystal
634 structure of nucleoplasmin-core: implications for histone binding and nucleosome
635 assembly. *Mol Cell*. 2001;8: 841–853.
- 636 39. Banuelos S, Hierro A, Arizmendi JM, Montoya G, Prado A, Muga A. Activation
637 mechanism of the nuclear chaperone nucleoplasmin: role of the core domain. *J Mol*
638 *Biol*. 2003;334: 585–593.
- 639 40. Salvany L, Chiva M, Arnan C, Ausio J, Subirana JA, Saperas N. Mutation of the small
640 acidic tract A1 drastically reduces nucleoplasmin activity. *FEBS Lett*. 2004;576: 353–
641 357.
- 642 41. Taneva SG, Banuelos S, Falces J, Arregi I, Muga A, Konarev P V, et al. A mechanism
643 for histone chaperoning activity of nucleoplasmin: thermodynamic and structural
644 models. *J Mol Biol*. 2009;393: 448–463.
- 645 42. Fernandez-Rivero N, Franco A, Velazquez-Campoy A, Alonso E, Muga A, Prado A. A
646 Quantitative Characterization of Nucleoplasmin/Histone Complexes Reveals
647 Chaperone Versatility. *Sci Rep*. 2016;6: 32114.
- 648 43. Namboodiri VM, Akey I V, Schmidt-Zachmann MS, Head JF, Akey CW. The
649 structure and function of *Xenopus* NO38-core, a histone chaperone in the nucleolus.
650 *Structure*. 2004;12: 2149–2160.
- 651 44. Ramos I, Fernandez-Rivero N, Arranz R, Aloria K, Finn R, Arizmendi JM, et al. The
652 intrinsically disordered distal face of nucleoplasmin recognizes distinct
653 oligomerization states of histones. *Nucleic Acids Res*. 2014;42: 1311–1325.
- 654 45. Auer TO, Duroure K, De Cian A, Concordet JP, Del Bene F. Highly efficient
655 CRISPR/Cas9-mediated knock-in in zebrafish by homology-independent DNA repair.
656 *Genome Res*. 2014;24: 142–153.
- 657 46. Gagnon JA, Valen E, Thyme SB, Huang P, Akhmetova L, Pauli A, et al. Efficient

- 658 mutagenesis by Cas9 protein-mediated oligonucleotide insertion and large-scale
659 assessment of single-guide RNAs. *PLoS One*. 2014;9: e98186.
- 660 47. Li L, Baibakov B, Dean J. A subcortical maternal complex essential for
661 preimplantation mouse embryogenesis. *Dev Cell*. 2008;15: 416–425.
- 662 48. Xu Q, Wang F, Xiang Y, Zhang X, Zhao ZA, Gao Z, et al. Maternal BCAS2 protects
663 genomic integrity in mouse early embryonic development. *Development*. 2015;142:
664 3943–3953.
- 665 49. Dekens MP, Pelegri FJ, Maischein HM, Nusslein-Volhard C. The maternal-effect gene
666 futile cycle is essential for pronuclear congression and mitotic spindle assembly in the
667 zebrafish zygote. *Development*. 2003;130: 3907–3916.
- 668 50. Yabe T, Ge X, Pelegri F. The zebrafish maternal-effect gene cellular atoll encodes the
669 centriolar component sas-6 and defects in its paternal function promote whole genome
670 duplication. *Dev Biol*. 2007;312: 44–60.
- 671 51. Kimmel CB, Ballard WW, Kimmel SR, Ullmann B, Schilling TF. Stages of embryonic
672 development of the zebrafish. *Dev Dyn*. 1995;203: 253–310.

673
674

675 **Figure legends**

676 **Figure 1: Consensus phylogenetic tree of Npm2 proteins.**

677 This phylogenetic tree was constructed based on the amino acid sequences of Npm2 proteins
678 (for the references of each sequence see Supplemental Table S1) using the Neighbour Joining
679 method with 1,000 bootstrap replicates. The number shown at each branch node indicates the
680 bootstrap value (%). The tree was rooted using Npm3 and Npm1 sequences. The Npm2a
681 sequences are in blue, the Npm2b sequences are in red, the salmonid Npm2b1 sequences are
682 in purple, and the salmonid Npm2b2 sequences are in pink.

683 **Figure 2: Conserved genomic synteny of *npm2* genes.**

684 Genomic synteny maps comparing the orthologs of *npm2a*, *npm2b*, and their neighbouring
685 genes. *npm2* genes are named as *npm2a* and *npm2b* (formerly known as *npm2*). The other
686 genes were named after their human orthologs according to the Human Genome Naming
687 Consortium (HGNC). Orthologs of each gene are shown in the same color. The direction of
688 arrows indicates the gene orientation, with the ID of the genomic segment indicated above
689 and the position of the gene (in 10^6 base pairs) indicated below. The full gene names and
690 detailed genomic locations are given in Supplemental Table S3.

691 **Figure 3: Current status and proposed evolutionary history of *npm2* genes among**
692 **gnathostomes.**

693 The names of the current representative species of each phylum are given at the end of the
694 final branches, together with a red and/or blue X to denote the *npm2* genes they possess
695 (*npm2a*=red, *npm2b*=blue). The black X upon an *npm2* gene symbol indicates a gene loss.
696 LGD: local gene duplication; TGD: teleost-specific whole genome duplication; SaGD:
697 salmonid-specific whole genome duplication.

698 **Figure 4: Tissue distribution of *npm2a* and *npm2b* in different species.**

699 **A)** Tissue expression analysis by QPCR of *npm2a* and *npm2b* mRNAs in zebrafish and
700 *Xenopus*. **(B)** Expression level is expressed as a percentage of the expression in the ovary for
701 the most expressed gene. Data were normalized using *18S* expression. **(C-J)** Tissue
702 expression level by RNA-Seq of *npm2a* and *npm2b* mRNAs in different fish species. mRNA
703 levels are expressed in read per kilobase per million reads (RPKM). In salmonids **(I and J)**,
704 the two 4R isoforms of *npm2b* are *npm2b1* and *npm2b2*. Br, brain ; Gi, gills ; Lu, lung ; In,
705 intestine ; Li, liver ; Mu, muscle □ ; He, heart ; Bo, bone ; Ki, kidney ; Ov, ovary ; and Te,
706 testis.

707 **Figure 5: *npm2a* and *npm2b* expression during oogenesis and early development.**

708 QPCR analysis of (A) *npm2a* and (B) *npm2b* expression during oogenesis and early
709 embryonic development in zebrafish. Data were normalized using luciferase, and relative
710 expression was based on *npm2b* expression at the indicated stage. UF, unfertilized egg; hpf,
711 hours post-fertilization.

712 **Figure 6: CRISPR/cas9 knockout of *npm2a* and *npm2b* in zebrafish.**

713 (A) Relative expression level of *npm2a* and *npm2b* transcripts by QPCR in the fertilized
714 zebrafish eggs from crosses between *npm2a* or *npm2b* mutant female and wildtype (WT)
715 male, respectively. (B) Developmental success as measured by the proportion of fertilized
716 eggs that underwent normal cell division and reached normal developmental milestones
717 based on Kimmel et al. [51] from crosses between WT animals (control), and *npm2a* or
718 *npm2b* mutant female and WT male at 1 and 4 hours post-fertilization (hpf). Shaded grey
719 columns denote normal morphology and black columns denote abnormal morphology of the
720 fertilized eggs at 1 hpf. (C) Representative images demonstrating development of fertilized
721 eggs from crosses between control animals (left panels), and *npm2a* (middle panels) or
722 *npm2b* (right panels) mutant female and WT male at 64-cell, oblong, dome, germ ring, and
723 24-somite stages according to Kimmel et al [51]. N=3 for *npm2a* mutant and N=4 for *npm2b*
724 mutant. All assessments were performed from at least 3 clutches from each mutant. Scale
725 bars denote 500 nm. Red dotted lines define the diameter of the embryo. ** p<0.01,
726 ***p<0.001, ****p<<0.0001

727 **Supplemental Figure S1: Npm2a and Npm2b protein domain conservation.**

728 Presence of the Npm core (red color bar) and acidic tract (blue color bar) domains in *npm2a*
729 and *npm2b* types in various vertebrate species.

730 **Supplemental Figure S2: Genotyping by PCR for *npm2a* and *npm2b* in F1 embryos.**

731 *npm2a* and *npm2b* knockout animals were crossed with wildtype (WT) zebrafish, and
732 individual F1 embryos were harvested at 6 hours post-fertilization and subjected to

733 genotyping by PCR with gene-specific primers. The wildtype PCR product for *npm2a* was
734 1634 base pairs (bp) and the CRISPR/cas9-targeted knockout mutant band was 240 bp while
735 the WT *npm2b* band was 813 bp and the CRISPR/cas9-targeted knockout mutant band was
736 560 bp. The yellow asterisks denote the embryos carrying the mutant allele.

737 **Supplementary Data**

738 **Supplemental Table S1:** list of Npm2 protein sequences used in the phylogenetic analysis.

739 **Supplemental Table S2:** Npm2a and Npm2b protein sequence comparisons.

740 **Supplemental Table S3:** list of the genes from the conserved syntenic region of *npm2* genes.

741 **Supplemental Table S4:** Estimation of the ratio of substitution rates (dN/dS) in *npm2a* and
742 *npm2b* genes.

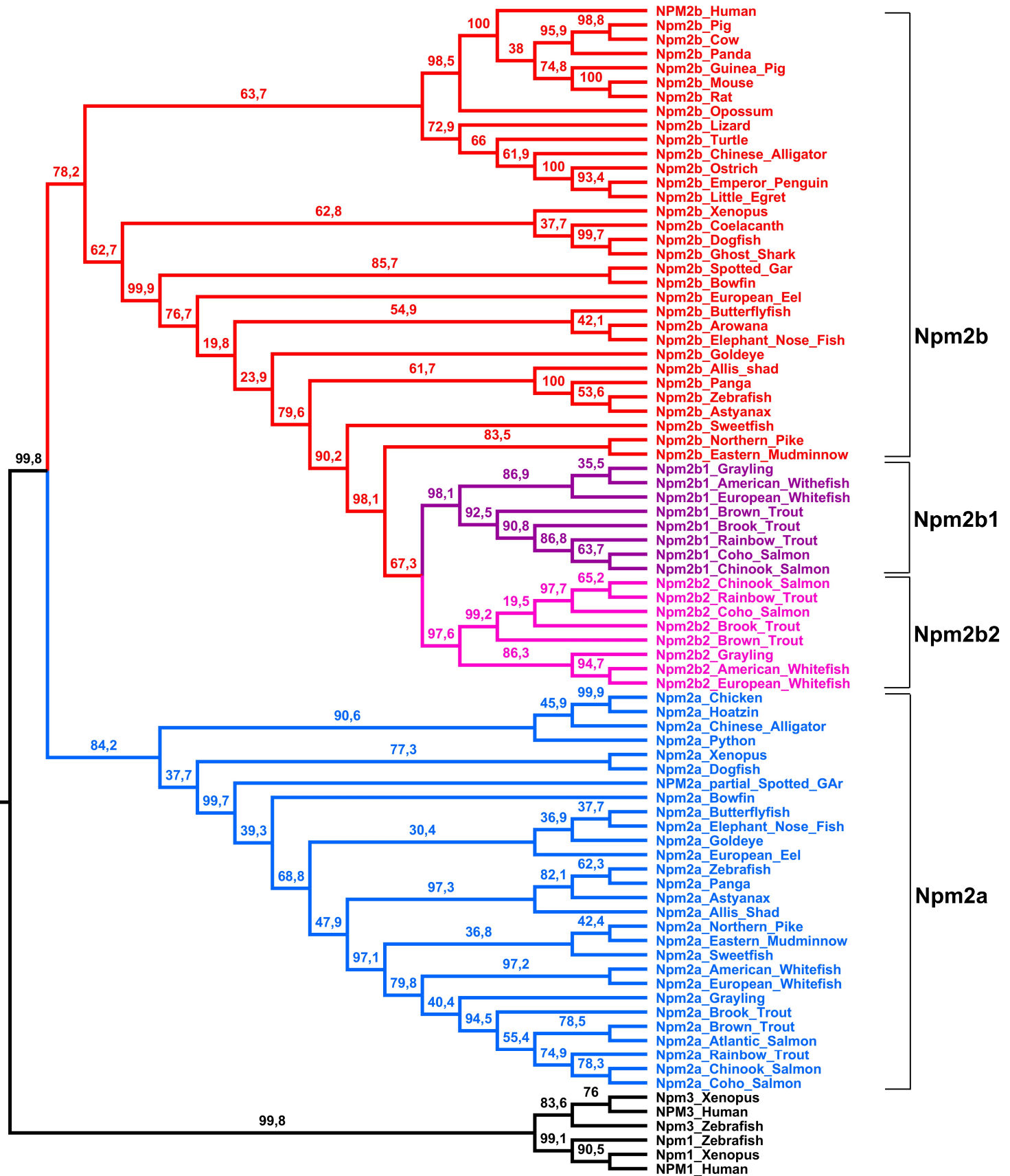
743 **Supplemental Table S5:** QPCR and PCR primers.

744 **Supplemental Fig.S1:** Npm2a and Npm2b protein domain conservation.

745 **Supplemental Fig.S2:** Genotyping of F1 embryos from *npm2a* and *npm2b* mutants.

Figure 1

Version preprint



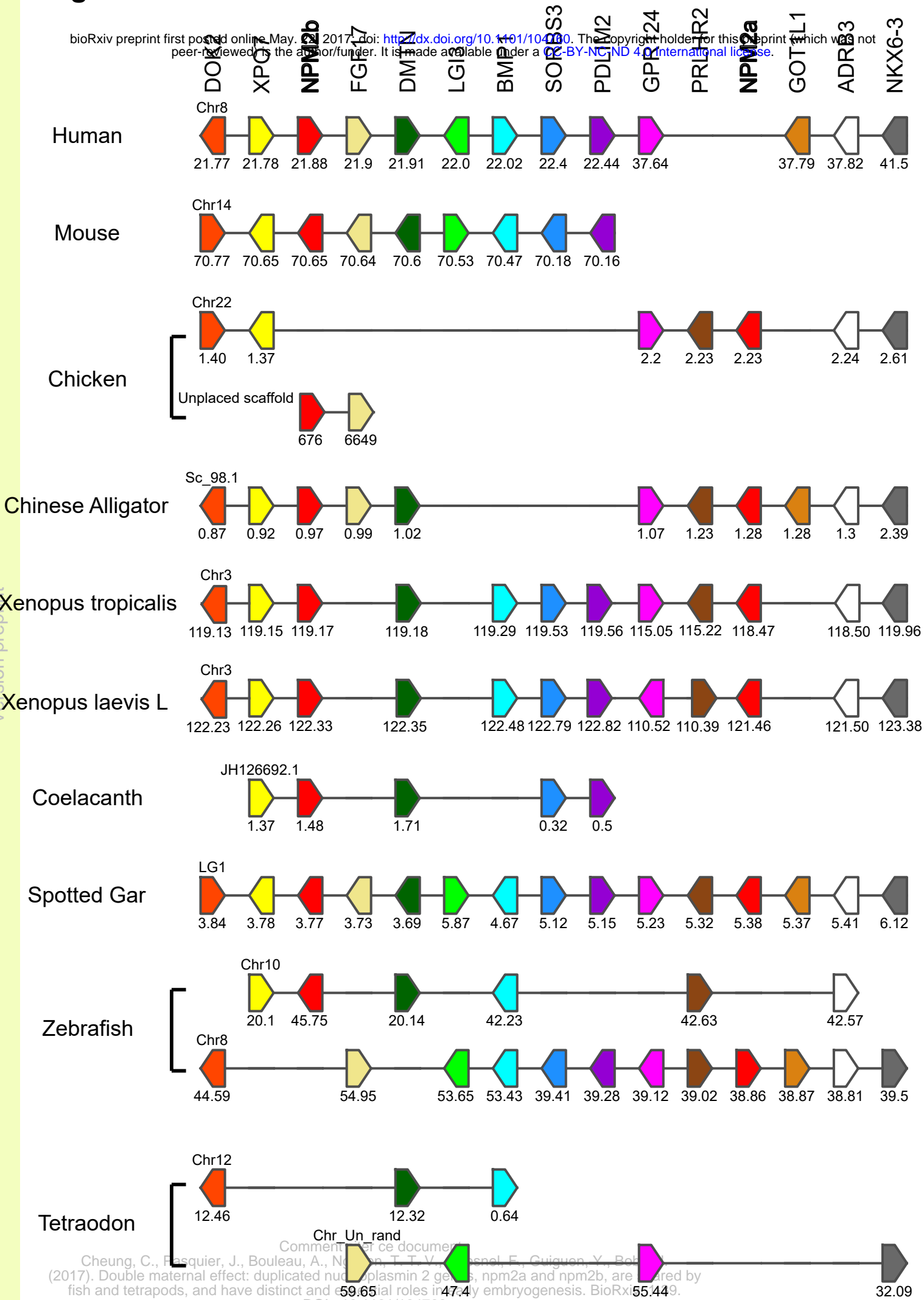
Comment citer ce document :

Cheung, C., Pasquier, J., Bouleau, A., Nguyen, T. T. V., Chesnel, F., Guiguen, Y., Bobe, J. (2017). Double maternal effect: duplicated nucleoplasm 2 genes, npm2a and npm2b, are shared by fish and tetrapods, and have distinct and essential roles in early embryogenesis. *BioRxiv*, 1-39.

DOI : 10.1101/104760

Figure 2

bioRxiv preprint first posted online May 24, 2017. doi: <https://doi.org/10.1101/104760>. The copyright holder for this preprint (which was not certified by peer review) is the author/funder. It is made available under aCC-BY-NC-ND 4.0 International license.



Cheung, C., Pasquier, J., Bouleau, A., Nguyen, T. T. V., Gagnon, E., Guignon, Y., Bokil, S. (2017). Double maternal effect: duplicated nucleoplasmin 2 genes, npm2a and npm2b, are shared by fish and tetrapods, and have distinct and crucial roles in early embryogenesis. *BioRxiv*: 151499. DOI: 10.1101/104760

Version preprint

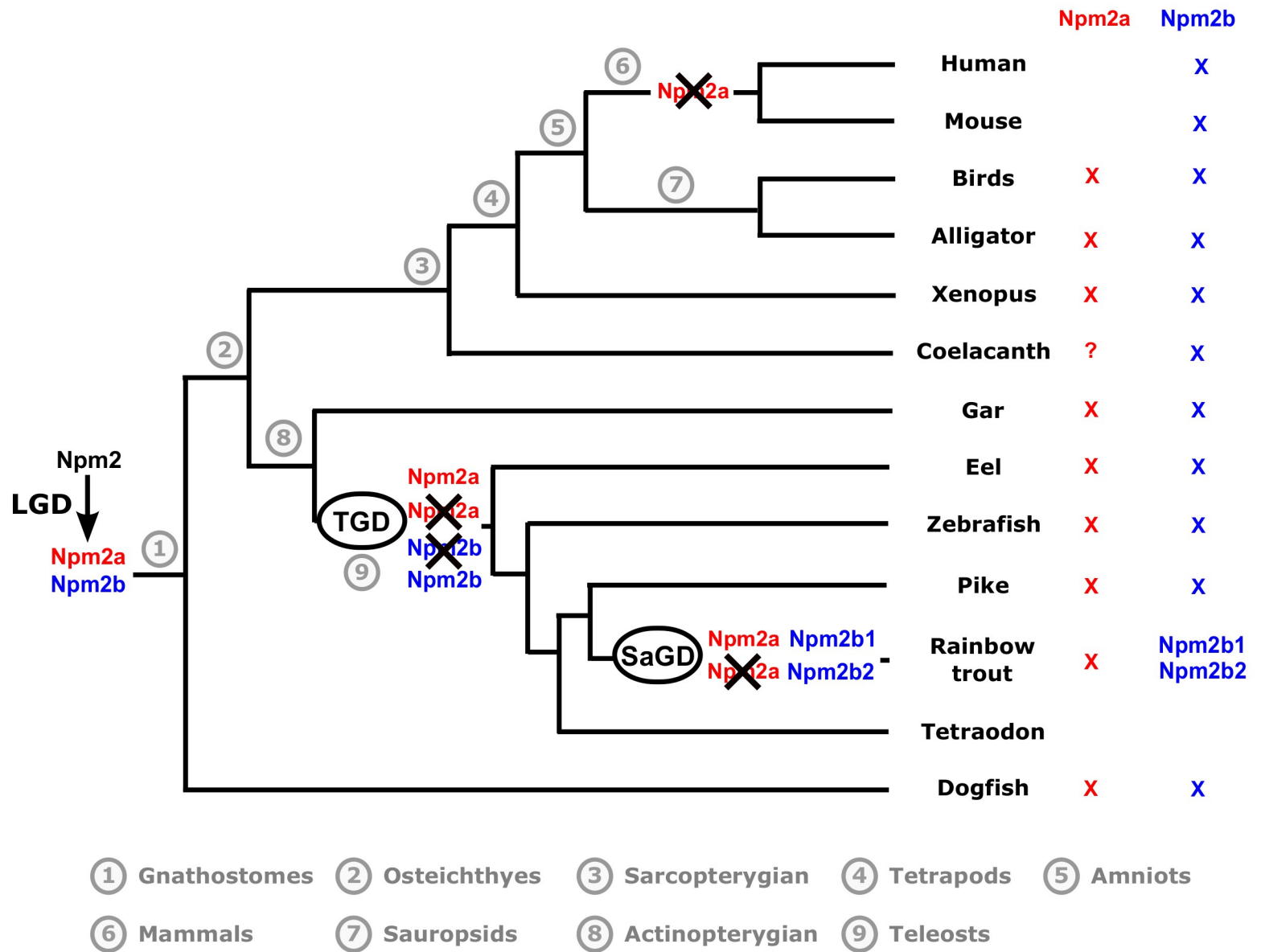


Figure 4

bioRxiv preprint first posted online May 22, 2017; doi: <http://dx.doi.org/10.1101/104760>. The copyright holder for this preprint (which was not certified by peer review) is the author/funder. It is made available under aCC-BY-NC-ND 4.0 International license.

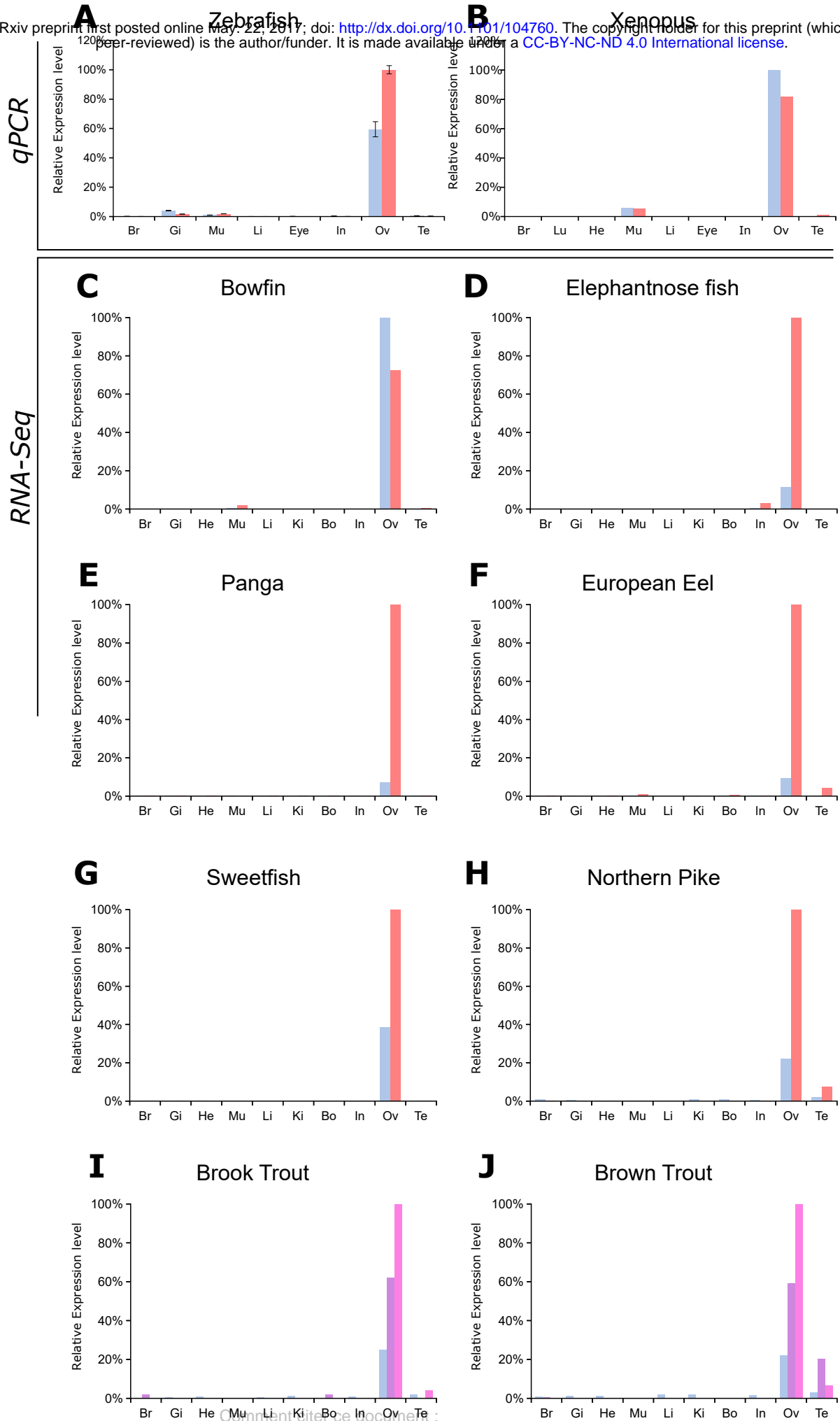


Figure 5

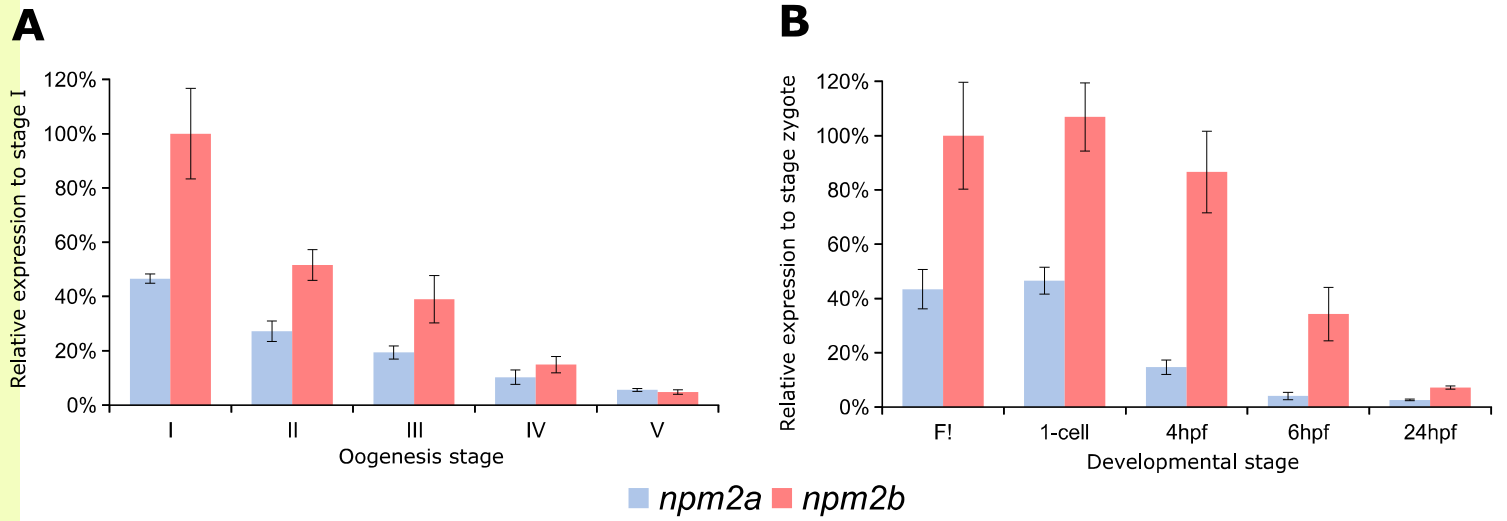
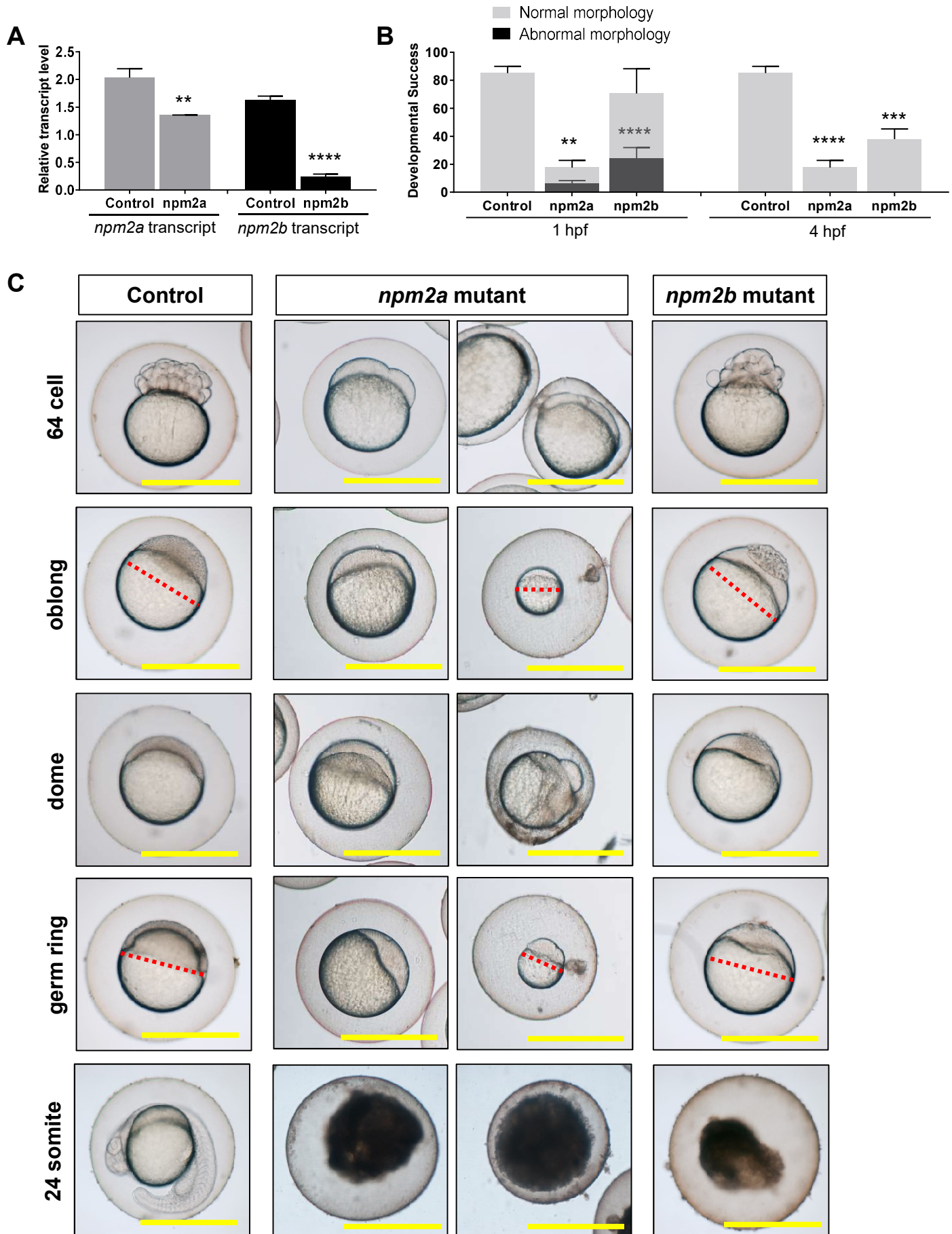
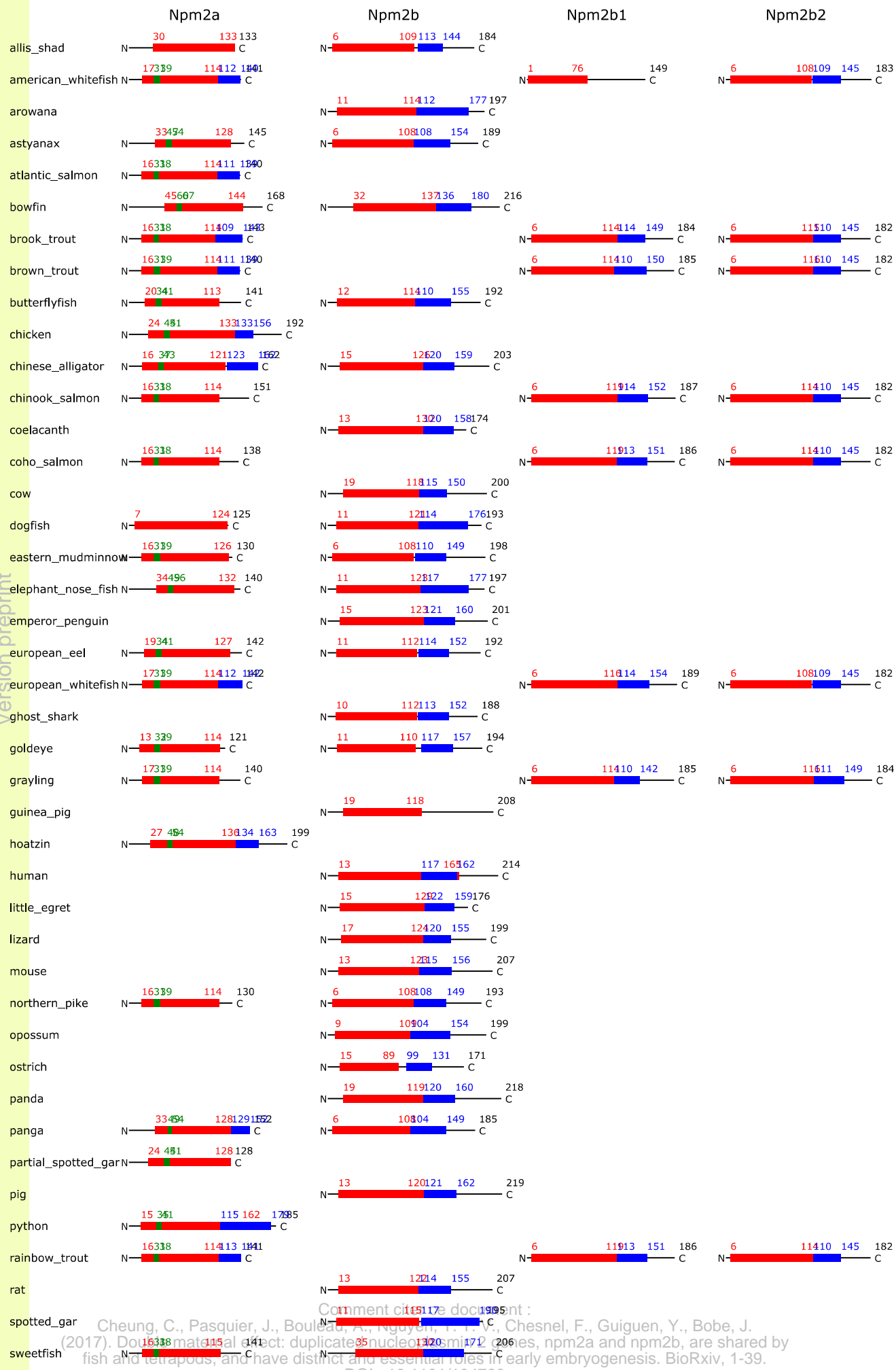


Figure 6



Supplemental Figure S1



Version preprint

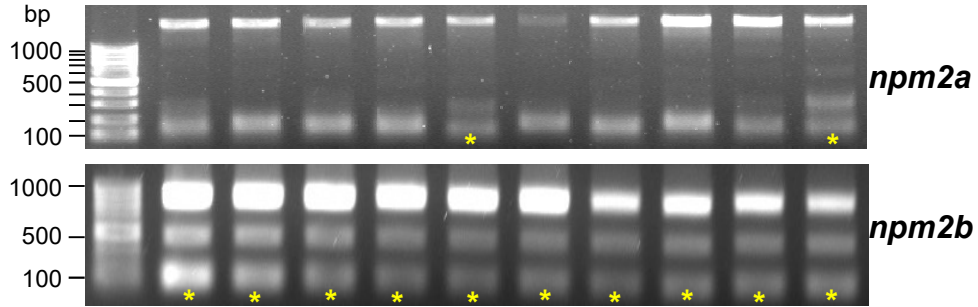
Comment on this document:

Cheung, C., Pasquier, J., Bouleau, A., Nguyen, T. T. V., Chesnel, F., Guiguen, Y., Bobe, J. (2017). Do not mistake the effect: duplicate nucleotides in nrm2b1 and nrm2b2, are shared by fish and tetrapods, and have distinct and essential roles in early embryogenesis. BioRxiv, 1-39.

DOI: 10.1101/158477

Supplemental Figures

S2



Comment citer ce document :

Cheung, C., Pasquier, J., Bouleau, A., Nguyen, T. T. V., Chesnel, F., Guiguen, Y., Bobe, J. (2017). Double maternal effect: duplicated nucleoplasmin 2 genes, *npm2a* and *npm2b*, are shared by fish and tetrapods, and have distinct and essential roles in early embryogenesis. *BioRxiv*, 1-39.

DOI : 10.1101/104760